Boron filling of high aspect ratio holes by chemical vapor deposition for solid-state neutron detector applications

Kuan-Chih Huang,[a] Rajendra Dahal, Nicolas LiCausi, and James J.-Q. Lu
Department of Electrical, Computer and Systems Engineering, Rensselaer Polytechnic Institute, 110 8th Street, Troy, New York 12180-3522

Yaron Danon
Department of Mechanical, Aerospace and Nuclear Engineering, Rensselaer Polytechnic Institute, 110 8th Street, Troy, New York 12180-3522

Ishwara B. Bhat
Department of Electrical, Computer and Systems Engineering, Rensselaer Polytechnic Institute, 110 8th Street, Troy, New York 12180-3522

(Received 24 May 2012; accepted 23 July 2012; published 9 August 2012)

A multiple deposition and etching process has been developed to enable high fill factor boron deposition in high aspect ratio holes fabricated in a (100) silicon substrate. The boron deposition was carried out using low-pressure chemical vapor deposition and the etching was done by inductively coupled plasma reactive ion etching technique. The boron deposition processes were carried out under different conditions in order to find a baseline process condition. The boron etching processes done under different conditions with the photoresist as the mask are also discussed. Finally, the fabricated neutron detector with the highest fill factor was characterized for the thermal neutron detection efficiency. © *2012 American Vacuum Society*. [http://dx.doi.org/10.1116/1.4742856]

I. INTRODUCTION

As neutrons are a very specific indicator of fissile materials, efficient solid-state neutron detectors based on silicon microstructures with large detecting surface area and low gamma sensitivity are urgently needed for border security and illicit nuclear material detection. Helium-3 gas-filled tube has long been used as a neutron detector because of its high neutron detection efficiency, but drawbacks, such as poor portability and high bias voltage, have resulted in increased research activities toward solid-state neutron detector.

Solid-state neutron detectors have been demonstrated by depositing a thin converter material, such as boron-10 (^{10}B) or lithium-6 fluoride (^{6}LiF), on top of Si or GaAs p–n junctions.[1–4] When an incident neutron interacts with ^{10}B, an alpha (α) particle and a lithium-7 (^{7}Li) ion are released according to[5]

$$^{10}_{5}\mathrm{B}+^{1}_{0}n \rightarrow \begin{cases} 6\%: & ^{7}_{3}\mathrm{Li}(1.015\,\mathrm{MeV})+^{4}_{2}\alpha(1.777\,\mathrm{MeV}) \\ & \mathrm{Q}=2.792\,\mathrm{MeV}\ (\mathrm{ground\ state}) \\ 94\%: & ^{7}_{3}\mathrm{Li}^{*}(0.840\,\mathrm{MeV})+^{4}_{2}\alpha(1.470\,\mathrm{MeV}) \\ & \mathrm{Q}=2.310\,\mathrm{MeV}\ (\mathrm{first\ excited\ state}). \end{cases}$$

The α and ^{7}Li particles lose their energy due to the impact ionization within the p–n junction and thus create electron–hole pairs (EHPs). The EHPs created inside the depletion region of the p–n junction are separated by the built-in electric field and then collected as current or voltage pulses by external circuits.

In order to maximize the probability of neutron interaction, the ^{10}B layer (density $\sim$2.35 g/cm^3) must be thick enough. For example, an $\sim$45 μm thick ^{10}B layer results in an interaction probability of 90%.[6] However, the ^{10}B layer must be thin enough (2–3 μm) to allow the generated α particles (1.47 MeV) to escape from the ^{10}B layer and then reach the p–n junction with enough energy. Otherwise, the α particles will be absorbed by the ^{10}B layer.[7] It is this contradiction of the ^{10}B layer thickness that limits the neutron detection efficiency of planar devices to 2%–5%.[3,8,9] To overcome this limitation and enhance the neutron detection efficiency, researchers have proposed to use perforated Si p–n junctions filled with ^{6}LiF or Si pillar structures filled with ^{10}B.[9,10] We have proposed boron filled high aspect ratio hexagonal/honeycomb holes and parallel trenches with continuous Si p^{+}–n junctions.[6] The basic working principle and the schematic of layer structure for a honeycomb type solid-state neutron detector are illustrated in Fig. 1. One of the challenges in the proposed design is to completely fill the high aspect ratio holes with boron. Deo *et al.* used low-pressure chemical vapor deposition (LPCVD) to conformally fill the gaps in a silicon micropillar structure having 6 to 1 aspect ratio with ^{10}B using B-enriched decaborane ($B_{10}H_{14}$) as the precursor.[11] This micropillar structure is easier to fill than the one proposed here as pillar structure allows adequate gas transport between the pillars. However, to conformally fill high aspect ratio holes is much more challenging.

In this work, LPCVD with diborane (B_2H_6) as the precursor gas was used. Our earlier Monte Carlo simulations showed that the honeycomb hole aspect ratio should be 40 to 2.8 (40 μm in depth and 2.8 μm in width) to get the highest neutron detection efficiency of 48%.[12] As neutron detection efficiency scales with the boron fill factor, a void-free boron filling process in the high aspect ratio holes is technically challenging and urgently required. This paper reports on a demonstration of boron filling of high aspect ratio holes using multiple deposition and etching process.

[a]Author to whom correspondence should be addressed; electronic mail: huangk6@rpi.edu

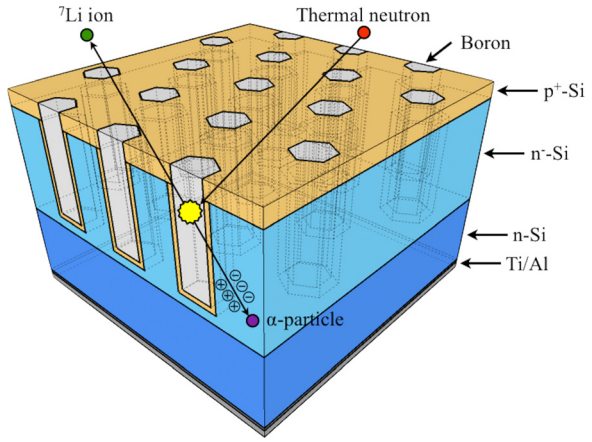

FIG. 1. (Color online) Schematic of layer structure and the basic working principle for a honeycomb type solid-state neutron detector (front side *p*-contact is hidden for clarity).

II. EXPERIMENTAL METHOD

A. Fabrication of high aspect ratio configurations

A 4 in. moderately doped *n*-type (100) silicon wafer (resistivity ~0.4 Ω cm) was used as a substrate for depositing an ~50 μm thick lightly doped *n*-type (~50 Ω cm) epitaxial layer, followed by an ~1 μm thick heavily doped *p*-type (~0.01 Ω cm) epitaxial layer. In our mask design, 16 dies can be processed on a 4 in. wafer at one time and each die contains 12 individual devices with different sizes. Individual devices in each die were isolated by mesa etching of the *p*-type layer using photolithography and reactive ion etching (RIE) with sulfur hexafluoride (SF_6) and oxygen (O_2) plasmas. To passivate the exposed mesa sidewalls, an ~1.5 μm thick silicon dioxide (SiO_2) layer was deposited everywhere. The 1.5 μm thick SiO_2 from the device area was then etched off using photolithography and wet buffered oxide etch (BOE), followed by the deposition of an ~300 nm thick SiO_2. This 300 nm thick SiO_2 was used as a boron etch stop layer later on in the device fabrication process. High aspect ratio hexagonal holes and parallel trenches were defined in the device area using photolithography, dry etching of the 300 nm thick SiO_2, and deep reactive ion etching (DRIE) of Si (using photoresist and the 300 nm thick SiO_2 as the mask) with a standard Bosch process.[13] Bosch process consists of many cycles of passivation layer deposition using C_4H_8 and silicon etching using SF_6. This alternating passivation and etching process can result in vertical sidewalls with high aspect ratio. The cross-sectional scanning electron microscope (SEM) images of the hexagonal holes and parallel tranches after DRIE are shown in Figs. 2(a) and 2(b), respectively. The inset in Fig. 2(a) shows the top view SEM image of the hexagonal holes. These Si wafers became the starting wafers for boron deposition with LPCVD.

B. Low-pressure chemical vapor deposition

LPCVD was selected because it has been shown to produce conformal Si thin films on very high aspect ratio structures using silane (SiH_4) as a precursor.[14] Based on this concept, the LPCVD experiments were designed with B_2H_6 instead of SiH_4 to deposit conformal boron films because B_2H_6 is a gas at room temperature allowing easy transport and has been extensively used as a dopant source in the epitaxial Si deposition.[15] In this work, diluted diborane (1% B_2H_6 in H_2) was used as a precursor to deposit boron films. Samples were placed on a silicon carbide coated graphite susceptor that was inductively heated to 525 °C in a cold-wall horizontal quartz reactor. A process pressure of 250 mTorr and a B_2H_6/H_2 flow rate of 50 SCCM (SCCM denotes cubic centimeters per minute at standard temperature and pressure) were kept during the boron deposition. For device layers, boron diffusion was first carried out at 900 °C for 30 min in the same reactor to get a continuous p^+-Si layer prior to filling the holes with boron.

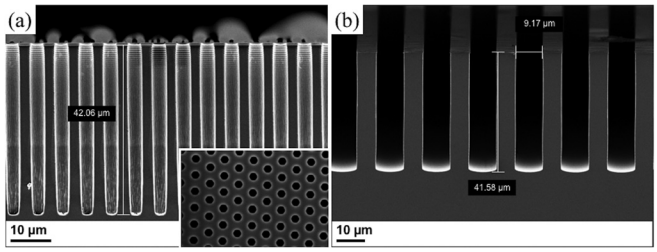

FIG. 2. Cross-sectional SEM images of (a) 42 μm deep and 3.8 μm wide hexagonal holes and (b) 41 μm deep and 9 μm wide parallel trenches, fabricated using DRIE on silicon substrates. The inset in (a) shows the top view.

C. Inductively coupled plasma reactive ion etching

After the boron deposition, boron was etched using inductively coupled plasma (ICP) reactive ion etching (RIE) (Trion Phantom III Reactive Ion Etch System) with SF_6/O_2 plasmas. Similar work using electron cyclotron resonance plasma etching has shown promising results for boron etching.[16] In this work, two optimized ICP-RIE conditions were found to be stable and used to carry out an isotropic etching and an anisotropic etching for different purposes. The isotropic etching was designed to remove boron from the neck of the incompletely filled holes and the anisotropic etching was used to open windows for *p*-contact metallization after completing the boron deposition process. The isotropic etching was done with a pressure of 500 mTorr, an SF_6 flow rate of 45 SCCM, and an O_2 flow rate of 90 SCCM. The RIE power was maintained at 100 W and the ICP power, used to increase the etching plasma density, was held at 200 W. The anisotropic etching was conducted with a pressure of 120 mTorr, an SF_6 flow rate of 20 SCCM, and an O_2 flow rate of 40 SCCM. The RIE and ICP power were kept at 200 and 600 W, respectively. The results are shown and discussed in Sec. III.

D. Multiple deposition and etching process

A single step boron deposition process in high aspect ratio holes resulted in a large void inside the hole due to the nonuniform deposition rate with depth. In order to minimize the void size, a multiple deposition and etching process was designed and used. In this process, LPCVD was used to deposit boron into 2–3 μm wide holes until ~1 μm wide holes

remained. These partially filled holes were then spin-coated with photoresist, exposed, and then developed. It was found that the photoresist was developed on the top but intact inside the holes due to the reentrant profile of the boron film on the sidewalls of the holes. This remaining photoresist was used as the mask during the isotropic ICP-RIE. After boron was etched from the top and the necks of the holes, the remaining photoresist was removed and the boron deposition was conducted again. Additional boron deposition and etching processes were carried out repeatedly until the highest fill factor was reached. Once the highest fill factor was reached, boron film on top of the substrate was removed using the anisotropic ICP-RIE until the SiO_2 etch stop layer was exposed. The SiO_2 layer was then removed using BOE to expose p^+-Si for metallization. An ~1 μm thick aluminum (Al) with 2% Si was sputtered on the front side for *p*-contact and a 100 nm thick titanium followed by a 900 nm thick Al were sputtered on the back side for *n*-contact. The finished wafers were diced into single dies, which were wire-bonded to flat packs for electrical and thermal neutron detection efficiency measurements.

III. RESULTS AND DISCUSSION

A. Boron filling process with LPCVD

In order to find an optimum condition for boron deposition, the growth temperature and the process pressure were varied. The parameters of interest were the growth rate as well as the conformal coverage ratio, defined as the ratio of the boron film thickness on the bottom of the sidewall to the thickness on top of the sidewall. The conformal coverage ratios were characterized using cross-sectional SEM images. Figures 3(a) and 3(b), respectively, show the growth rate and the conformal coverage ratio as a function of temperature for the parallel trench structure with a process pressure of 320 mTorr and a B_2H_6/H_2 flow rate of 80 SCCM. Growth rate has two distinct regimes: reaction rate limited regime (below ~600 °C) and mass transport limited regime (above ~600 °C). In the reaction rate limited regime, growth rate follows an Arrhenius relationship with an activation energy of ~26.12 kJ/mol and finally becomes relatively independent of temperature in the mass transport limited regime as shown in Fig. 3(a). The growth rate as a function of temperature for B_2H_6 is similar to that for SiH_4 in silicon epitaxial growth process.[17] However, the conformal coverage ratio decreases as the temperature was increased from 500 to 600 °C as shown in Fig. 3(b). Increasing the temperature from 600 to 700 °C yielded a relatively large decrease in conformal coverage ratio. Therefore, deposition below the 600 °C transition point was found to be ideal because it allows for a reasonable growth rate while still achieving a high conformal coverage ratio. Besides, the effects of process pressure on the growth rate and the conformal coverage ratio were also studied and the results are shown in Fig. 4. Temperature was maintained at 600 °C with a B_2H_6/H_2 flow rate of 50 SCCM. When the pressure was decreased from 480 to 300 mTorr, conformal coverage ratio was improved to approximate 75% with a corresponding decrease in the growth rate.

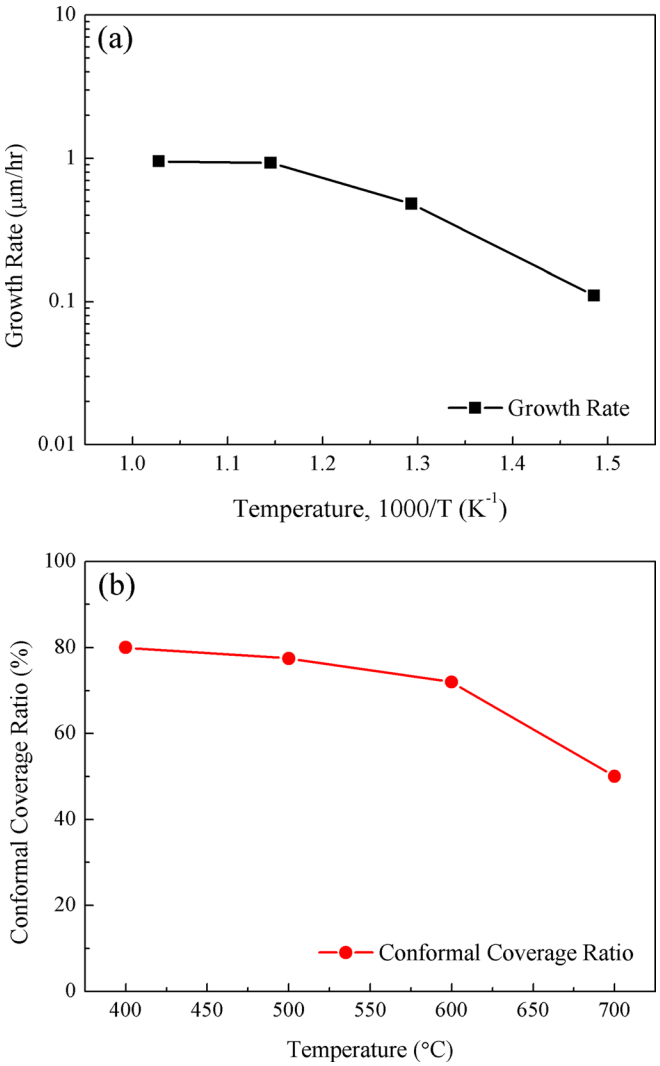

FIG. 3. (Color online) (a) Effect of growth temperature on the growth rate and (b) the effect of growth temperature on the conformal coverage ratio with a process pressure of 320 mTorr and a B_2H_6/H_2 flow rate of 80 SCCM in the parallel trench structure.

Although pressure plays an important role, temperature plays a more critical role in maximizing the conformal coverage ratio. These results suggest that the boron deposition must be done in the reaction rate limited regime with a low pressure (less than 300 mTorr) to achieve a conformal coverage ratio (more than 80%). Based on these results, 525 °C, 250 mTorr, and 50 SCCM were selected as a baseline growth temperature, process pressure, and B_2H_6/H_2 flow rate, respectively, to deposit boron into the hexagonal holes.

Three series of samples, T-1 (parallel trenches), H-1, and H-2 (hexagonal holes), were investigated in this study. Samples were filled with boron using baseline growth temperature, process pressure, and B_2H_6/H_2 flow rate. The deposition times of T-1 and H-2 are 4 h and the deposition time of H-1 is 8 h. Detailed process conditions are listed in Table I. Figure 5 shows the cross-sectional SEM images of the boron film deposited in parallel trenches [Fig. 5(a)] and hexagonal holes [Figs. 5(b) and 5(c)]. Conformal coverage ratio of 79% has been demonstrated for the parallel trench

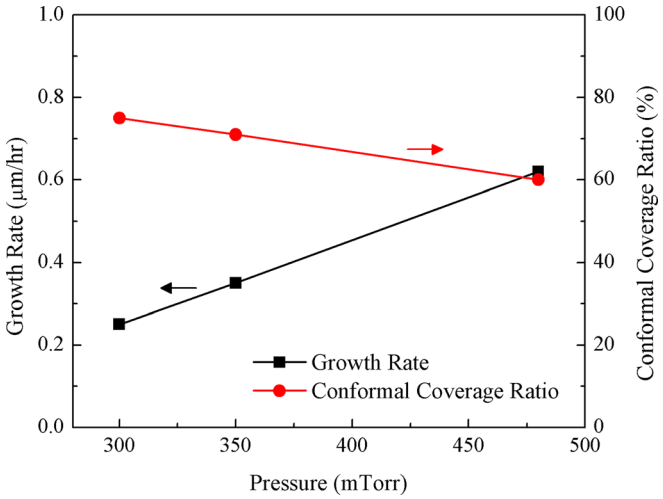

FIG. 4. (Color online) Effects of process pressure on the growth rate and the conformal coverage ratio with a substrate temperature of 600 °C and a B_2H_6/H_2 flow rate of 50 SCCM in the parallel trench structure.

structure (T-1). However, it was only 38% for the hexagonal hole structure under the same boron deposition condition (H-2). This is due to the difficulties in delivering precursor gases into the holes and removing reaction by-products from the holes compared to the trenches. H-1 and H-2 manifested that longer deposition time did not appreciably increase the boron film thickness, especially deep inside the holes. Besides, longer deposition time made the conformal coverage ratio become even lower (31%) (H-1). As the hole diameter at the top became ~1 μm while the deposition process was proceeding, the transport of B_2H_6 gas inside the hole and the removal of the reaction by-products might become more difficult. Hence, 4 h was selected as the baseline deposition time before the next deposition.

B. Boron etching process with ICP-RIE

ICP-RIE was used to etch boron isotropically using the pressure of 500 mTorr, SF_6 flow rate of 45 SCCM, and O_2 flow rate of 90 SCCM. The RIE and ICP power were maintained at 100 and 200 W, respectively. Our initial studies showed that ICP-RIE etched boron from the top as well as from the bottom of the holes. To prevent etching boron from inside the holes, photoresist was used as a mask. To fill the holes with photoresist, the wafer was spin-coated using two spin speeds, 500 rpm followed by 2000 rpm, and results are shown in Fig. 6(a). After performing a flood exposure and development, the photoresist above the boron necks was removed, whereas the photoresist below the boron necks still remained as shown in Fig. 6(b). Isotropic ICP-RIE with the photoresist coating allowed the etching of boron on top and

TABLE I. Details of the boron deposition conditions, boron thickness on the sidewalls, conformal coverage ratios, and boron fill factors for the samples T-1, H-1, and H-2.

Sample	Deposition time (h)	B thickness on top of the sidewall (nm)	B thickness on bottom of the sidewall (nm)	Conformal coverage ratio (%)	Boron fill factor (%)
T-1	4	3400	2700	79	67
H-1	8	850	260	31	72
H-2	4	650	250	38	70

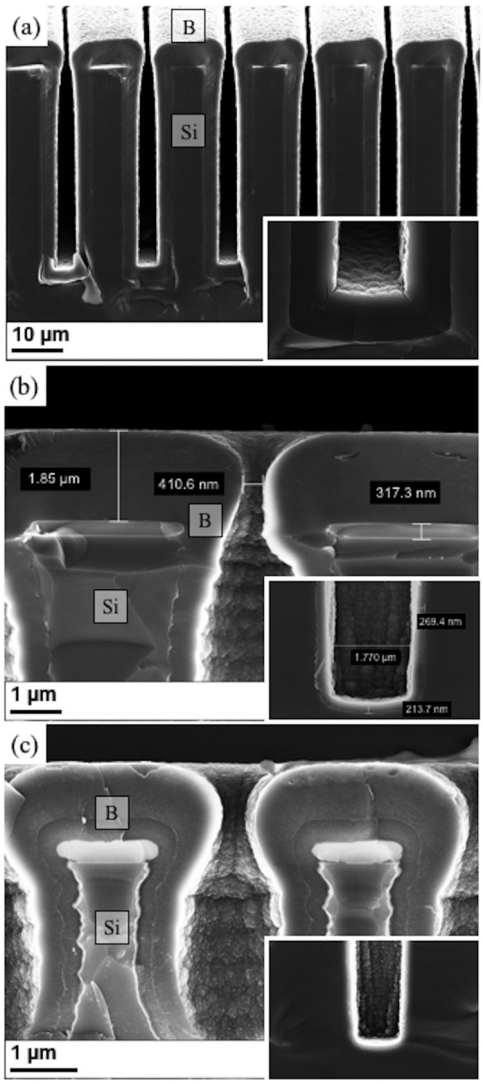

FIG. 5. Cross-sectional SEM images of the boron film deposited with a B_2H_6/H_2 flow rate of 50 SCCM for (a) 4 h in parallel trenches (T-1), (b) 8 h in hexagonal holes (H-1), and (c) 4 h in hexagonal holes (H-2). The insets show the cross section at the bottom of the microstructure.

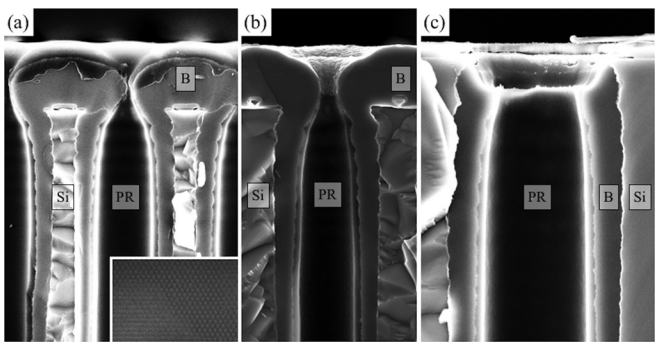

FIG. 6. Cross-sectional SEM images of the boron film after (a) the photoresist coating, (b) the flood exposure and development, and (c) the boron etching. The inset in (a) shows the top view.

near the neck of the holes without etching the boron inside the holes. The result is shown in Fig. 6(c). Figure 7(a) shows the cross-sectional SEM image of the boron film after isotropic ICP-RIE without the photoresist coating. Figures 7(b) and 7(c) show the cross-sectional SEM images of the boron film after isotropic ICP-RIE and anisotropic ICP-RIE, respectively, with the photoresist coating. Without the photoresist coating, almost all of the boron was etched off. On the contrary, the boron inside the holes was not etched at all with the photoresist coating. Only boron necks and the boron outside of the holes were etched. Isotropic etching is nondirectional and resulted in more etching on the boron necks as shown in Fig. 7(b). The wafer after the isotropic etching was utilized for further boron deposition. Anisotropic etching is directional and caused less etching on the boron necks as shown in Fig. 7(c). This anisotropic etching was used to etch boron from the top surface for making front side *p*-contact without etching boron from the neck region of the holes.

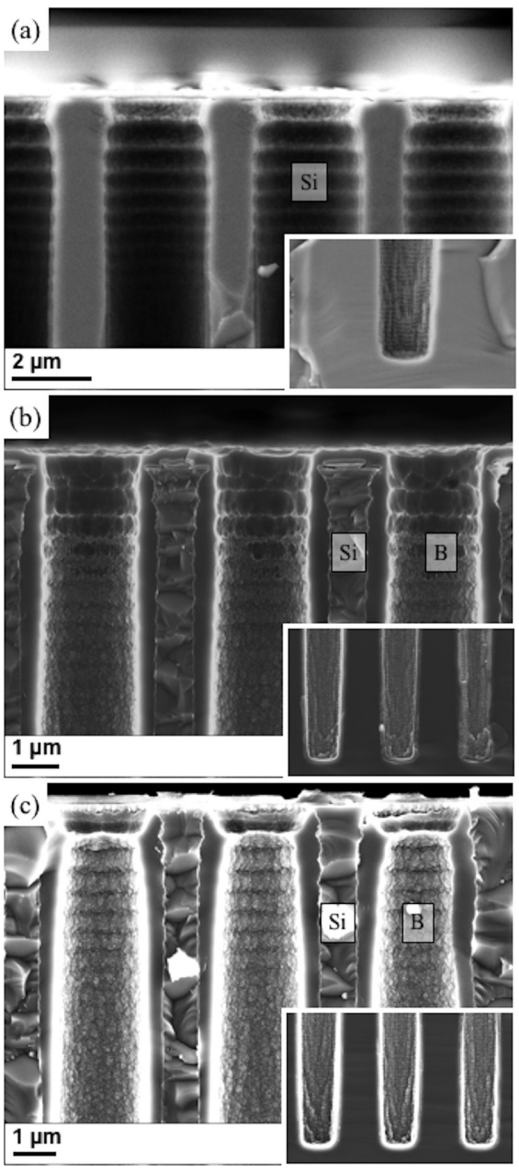

FIG. 7. Cross-sectional SEM images of the boron film after (a) the boron etching without the photoresist coating, (b) the isotropic ICP-RIE with the photoresist coating, and (c) the anisotropic ICP-RIE with the photoresist coating.

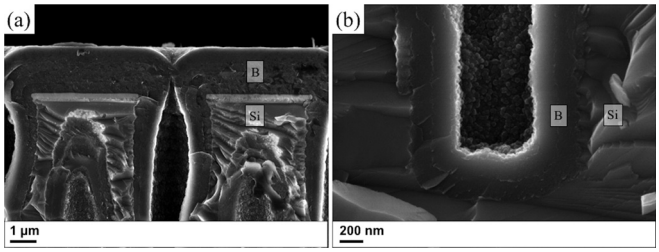

FIG. 8. Cross-sectional SEM images of the boron film after the second boron deposition: (a) top of the hole and (b) bottom of the hole.

C. Multiple deposition and etching process for fabricating a solid-state neutron detector

Boron fill factor is defined as the ratio of the boron filled volume to the total volume of the hole. The boron fill factors were characterized using cross-sectional SEM images. To improve the fill factor further, an additional deposition step was carried out after etching boron from the neck region of the holes. The fill factor inside the holes was improved from 83%, after the first deposition shown in Fig. 5(c), to 93%, after the second deposition shown in Fig. 8. With this high fill factor, the neutron detection efficiency is expected to be significantly higher. A 2 by 2 mm^2 detector with 2.3 μm wide and 37 μm deep hexagonal holes filled with natural boron (19.9% ^{10}B) and 1.5 μm wide silicon walls shows the best performance to date. Thermal neutron detection efficiency of $4.5 \pm 0.5\%$ was measured with an uncollimated neutron beam from a californium (^{252}Cf) source placed in a moderator housing.[18] Three separate measurements were taken and the results are shown in Fig. 9. One was measured with the ^{252}Cf source placed in the moderator housing (black curve labeled as 1), another one was measured with the ^{252}Cf source placed in the moderator housing and a 2 mm thick

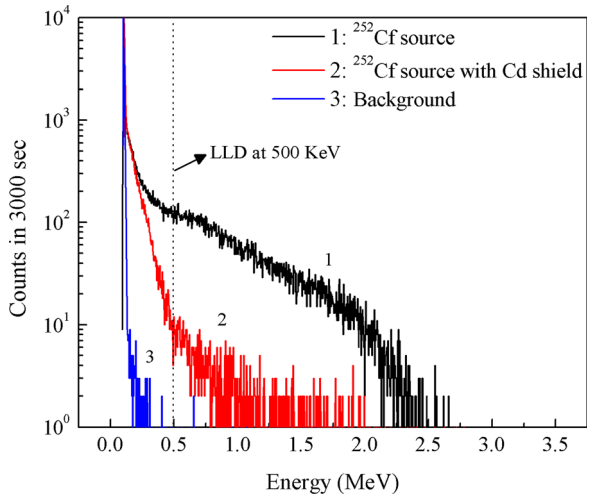

FIG. 9. (Color online) Measured pulse height distribution of the 2 by 2 mm^2 detector. The counts were recorded for 3000 s and the low level of detection was set at 500 keV while determining the thermal neutron detection efficiency.

cadmium (Cd) shield placed between the detector and the moderator (red curve labeled as 2), and the other one was measured with the ^{252}Cf source removed from the room (blue curve labeled as 3). Cd was used to block thermal neutrons and allow gamma rays and fast neutrons to pass. We have used natural diborane in our initial experiments due to the high cost of enriched diborane (99% ^{10}B). Higher efficiency could be achieved with the use of enriched diborane and a more accurate size and depth control of the high aspect ratio holes.

IV. CONCLUSIONS

Boron filling with high fill factor of 93% was achieved using a multiple deposition and etching process. An LPCVD with B_2H_6 as the precursor and an ICP-RIE with SF_6/O_2 plasmas were developed and used for the boron deposition and etching processes, respectively. Photoresist was used as the mask inside the holes during the etching process. In high aspect ratio (37 to 2.3) holes, up to 93% boron fill factor was achieved. With this high fill factor, the fabricated 2 by 2 mm^2 device showed neutron detection efficiency of $4.5 \pm 0.5\%$ with natural boron. The results are very promising for the fabrication of solid-state neutron detector with high neutron detection efficiency.

ACKNOWLEDGMENTS

The authors would like to thank the support and input of the support staff of the Rensselaer Polytechnic Institute Micro-Nano-Clean-Room (RPI MNCR) and Cornell Nano-Scale Science & Technology Facility (CNF). This work is supported by the joint NSF/DNDO Academic Research Initiative, Award No. CBET-0736104.

[1]C. Petrillo, F. Sacchetti, O. Toker, and N. J. Rhodes, Nucl. Instrum. Methods Phys. Res. A **378**, 541 (1996).
[2]D. S. McGregor, R. T. Klann, H. K. Gersch, and J. D. Sanders, Nucl. Sci. Symp. Conf. Rec. **1**, 2454 (2002).
[3]R. J. Nikolic, C. L. Cheung, C. E. Reinhardt, and T. F. Wang, Proc. SPIE **6013**, 601305 (2005).
[4]A. N. Caruso, J. Phys.: Condens. Matter **22**, 443101 (2010).
[5]G. F. Knoll, *Radiation Detection and Measurement* (Wiley, Hoboken, NJ, 2000).
[6]N. LiCausi, J. Dingley, Y. Danon, J. Q. Lu, and I. B. Bhat, Proc. SPIE **7079**, 707908 (2008).
[7]N. Tsoulfanidis, *Measurement and Detection of Radiation* (Taylor & Francis, Washington, 1995).
[8]A. Rose, Nucl. Instrum. Methods **52**, 166 (1967).
[9]J. K. Shultis and D. S. McGregor, IEEE Trans. Nucl. Sci. **53**, 1659 (2006).
[10]R. J. Nikolic, A. M. Conway, C. E. Reinhardt, R. T. Graff, T. F. Wang, N. Deo, and C. L. Cheung, Appl. Phys. Lett. **93**, 133502 (2008).
[11]N. Deo, J. R. Brewer, C. E. Reinhardt, R. J. Nikolic, and C. L. Cheung, J. Vac. Sci. Technol. B **26**, 1309 (2008).
[12]J. Dingley, Y. Danon, N. LiCausi, J. Q. Lu, and I. B. Bhat, *2009 International Conference on Mathematics, Computational Methods & Reactor Physics*, Saratoga Springs, NY (unpublished).
[13]F. Laermer, A. Urban, and R. Bosch, *13th International Conference on Solid-State Sensors, Actuators and Microsystems* Stuttgart, Germany, 5-9 June, 2005 (IEEE, New York, 2005), Vol. 2, p. 1118.
[14]G. B. Raupp and T. S. Cale, Mater. Res. Soc. Symp. Proc. **334**, 471 (1994).
[15]J. Pejnefors, S. L. Zhang, H. H. Radamson, J. V. Grahn, and M. Ostling, J. Appl. Phys. **88**, 1655 (2000).
[16]L. F. Voss, C. E. Reinhardt, R. T. Graff, A. M. Conway, R. J. Nikolic, N. Deo, and C. L. Cheung, J. Electron. Mater. **39**, 263 (2010).
[17]F. C. Eversteyn, Philips Res. Rep. **29**, 4566 (1974).
[18]J. Clinton, "Optimization and characterization of a novel self powered solid state neutron detector," Ph.D. dissertation (Rensselaer Polytechnic Institute, Troy, NY, 2011).